Applied Catalysis B: Environmental 154–155 (2014) 134–141

Contents lists available at ScienceDirect

Applied Catalysis B: Environmental

journal homepage: www.elsevier.com/locate/apcatb

Catalytic oxidation of organic pollutants on pristine and surface nitrogen-modified carbon nanotubes with sulfate radicals

Hongqi Sun[a], ChungKeat Kwan[a], Alexandra Suvorova[b], Ha Ming Ang[a], Moses O. Tadé[a], Shaobin Wang[a,*]

[a] Department of Chemical Engineering and CRC for Contamination Assessment and Remediation of the Environment (CRC CARE), Curtin University, GPO Box U1987, Perth, WA 6845, Australia
[b] Centre for Microscopy, Characterisation and Analysis, The University of Western Australia, Crawley, WA 6009, Australia

ARTICLE INFO

Article history:
Received 18 November 2013
Received in revised form 12 January 2014
Accepted 8 February 2014
Available online 18 February 2014

Keywords:
Carbon nanotube
Nitrogen doping
Sulfate radicals
Metal free
Phenol decomposition

ABSTRACT

Employing metal-free nanocarbons or carbonaceous materials as a catalyst for environmental water remediation is a promising clean approach because the green carbon materials can completely prevent the potential toxic metal leaching and secondary contamination to water body. This study reports that pristine multi-walled carbon nanotubes (MWCNTs) can effectively activate peroxymonosulfate (PMS) and peroxydisulfate (or persulfate, perdisulfate, PDS) to produce sulfate radicals for oxidation of phenol solutions. Surface nitrogen modification was conducted by a facile synthesis via annealing MWCNTs with ammonium nitrate at a low temperature and the nitrogen modified MWCNTs (N-CNT) was characterized by a variety of techniques. It was found that surface nitrogen modification of MWCNTs produced different effects on PMS and PDS activation. N-CNT can significantly improve the phenol degradation with PMS, but decrease the degradation efficiency with PDS. Reaction kinetics and the mechanism in catalytic oxidation of phenol solutions with sulfate radicals over CNT-based materials were discussed.

1. Introduction

Sulfate radicals ($SO_4^{\bullet-}$), either produced from peroxymonosulfate (PMS, HSO_5^-) or peroxydisulfate (or persulfate, perdisulfate, PDS, $S_2O_8^{2-}$), can be a promising alternative to hydroxyl radicals ($OH^{\bullet}$) for advanced oxidation in aqueous solution. They not only present a higher redox potential (2.5–3.1 V vs. hydroxyl radicals of 2.7 V), but show a better flexibility to a broad pH range than hydroxyl radicals [1–3]. At first, the sulfate radicals were mainly generated by activation of PMS or PDS using metal ions, such as Co(II), Mn(II), Fe(II), Ru(III), and Ag(I), etc [4,5]. The challenges in such homogeneous processes are the reuse and the toxicity of the metal catalysts, as well as the associated secondary contamination to the environment. Metals, metal oxides and supported metal oxides as heterogeneous catalysts were then employed [6–11], however, metal leaching still cannot be completely avoided [12].

Nanostructured carbons (nanocarbons), such as carbon nanotubes (CNTs), graphene oxide (GO) and graphene, possessing high thermal conductivity, high theoretical specific surface area (SSA), unique carrier mobility, low-dimensional structure, sp^2-hybridized carbon configuration, have demonstrated to be effective in a variety of catalytic processes [13–15]. It would be fascinating to introduce carbon/nanocarbon into environmental catalysis as a metal-free catalyst for heterogeneous remediation of organic pollutants in water. In a previous study, we noticed that activated carbon was able to activate PMS at a moderate level [16]. Recently, for the first time, we observed that reduced graphene oxide (rGO) showed a higher activity in degradation of phenol, 2,4-chlorophenol and methylene blue, compared to Co_3O_4 prepared by thermal decomposition of cobalt nitrate [3]. On the other hand, GO did not show any activity. Proper modification of rGO materials can significantly improve the adsorptive and/or catalytic oxidation performance in removal of organic pollutants. It was found that highly porous rGO can be prepared by an activation process using CO_2 at high temperature. The activation can significantly increase the SSA of rGO from 200 to higher than 1200 m^2/g, and largely improve the catalytic performance. For rGO, 100% MB removal was achieved in 4.0 h, and the time was reduced to 1.0 h on the activated rGO by CO_2 activation [17]. More recently, we reported that chemically compositional modification of rGO by nitrogen doping (N-rGO) can dramatically improve the catalytic activity in oxidation of phenol solutions. Unmodified rGO was able to degrade 52.5% phenol in 3.0 h with sulfate radicals, while N-rGO managed to remove all phenol in 45 min

* Corresponding author. Tel.: +61 892663776.
E-mail addresses: h.sun@curtin.edu.au (H. Sun), shaobin.wang@curtin.edu.au, wangshao@vesta.curtin.edu.au (S. Wang).

http://dx.doi.org/10.1016/j.apcatb.2014.02.012
0926-3373/

[18]. With the comparative analysis, sp^2 carbon, nitrogen dopants, and the oxygen-containing functional groups were suggested to be the origins of the catalytic activity.

Carbon nanotubes are built from sp^2 carbon units in hexagonal networks as in a graphene sheet, and the pristine CNTs have very limited functional groups, such as –OH, –C=O, and –COOH, which can be enriched by an oxidation process using various acids, ozone, plasma or heat treatment [19]. In the oxidative dehydrogenation of *n*-butane, 88.9% of the converted butane was burnt, yielding 1.6% alkenes over pristine CNTs. When the CNTs were functionalized with oxygen containing groups by refluxing and oxidizing in concentrated HNO_3, the yield of alkenes was increased to 6.7% [20]. Yu et al. [21] reported that, in the selective aerobic oxidation of cyclohexane in liquid phase, CNTs displayed a reaction rate at 2–10 times higher than those of Au/ZSM-5 and FeAlPO catalysts. Luo et al. [13] reported that CNTs as metal-free catalysts exhibited an excellent activity in the selective oxidation of ethylbenzene to acetophenone in liquid phase with oxygen. It was found that CNTs played an important role in production of acetophenone through π–π interactions between the radical species, peroxide, and the graphene sheets of the CNTs. Moreover, surface carboxylic groups on the CNTs are unfavorable to ethylbenzene oxidation.

Nitrogen doping has been discovered to be very effective in enhancing the catalytic activities of CNTs. N-doped CNTs can be prepared by either in-situ doping during the synthesis or post-treatment of CNTs with nitrogen precursors. In-situ process can incorporate nitrogen into sp^2 carbon network (graphitic N), while post-treatment generally leads to the surface functionalization (pyridinic and pyrrolic N) [22]. In-situ synthesis of N-CNTs has been well developed, and a variety of nitrogen precursors, such as NH_3 [23], aniline [24], ethylene diamine [25], and acetonitrile [26] were employed to produce N dopants at a high temperature. Post-treatment at a low temperature would be cost-effective by employment of the commercially available CNTs, yet fails to incorporate nitrogen into sp^2 carbon networks.

Herein, we reported a facile nitrogen modification method of CNTs by thermal treatment of commercial CNTs with ammonium nitrate at a low temperature of 350 °C. Surface functionalization of CNTs was achieved by introduction of pyridinic and pyrrolic N, with bulk properties remaining unchanged. This material facilitated the mechanistic study in identification of the catalytically active sites of nanocarbons in producing sulfate radicals from PDS and PMS. For the first time, pristine CNTs and nitrogen modified CNTs (N-CNTs) were demonstrated effectively for catalytic degradation of phenol solutions with sulfate radicals. The activity of N-CNTs was comparable to N-doped rGO in activation of PMS for phenol oxidation.

2. Experimental

2.1. Materials and preparation of N-CNTs

Commercial MWCNTs were purchased from Chengdu Organic Chemicals, China. The products were prepared by chemical vapor deposition (CVD) using C_2H_4 as a carbon precursor and nickel based catalyst, and purified by refluxing in 6 mol/L hydrochloric acid for several hours. The CNTs have a diameter of 10–20 nm, a length of 30–100 μm, and a purity of >95% by weight. For preparation of N-CNTs, 1.0 g of CNTs and 1.0 g of ammonium nitrate were dissolved in 50 mL of ethanol, and the mixed solution was stirred for 30 min. Then solution temperature was raised to 50 °C to evaporate ethanol whilst stirring. The dried mixture was then put into a furnace for calcination at 300, 350 or 400 °C for 1 h at a heating rate of 5 °C/min, further washed by ethanol once and ultrapure water for three times, and N-CNT-30, N-CNT-35 and N-CNT-40 were then obtained, respectively. N-CNT-35 showed the highest activity so it was chosen for detailed characterization and further oxidation reactions.

2.2. Characterization of carbon materials

Raman spectra were recorded on an ISA (Dilor) dispersive Raman spectrometer with argon ion 514 nm lasers. X-ray diffraction (XRD) patterns were obtained on a Bruker D8-Advanecd X-ray diffractometer with Cu *K*α radiation (λ = 1.5418 Å), at accelerating voltage and current of 40 kV and 40 mA, respectively. Scanning electron microscopy (SEM) was performed on a Zeiss Neon 40EsB FIBSEM. Transmission electron microscopy (TEM) has been carried out using a JEOL 3000F field emission TEM. Quantification of chemical composition was carried out using electron energy loss spectroscopy (EELS) on the TEM. Chemical states of elements were also analyzed by X-ray photoelectron spectroscopy (XPS) using Thermo Escalab 250 with a monochromatic Al *K*α X-ray source. All binding energies were calibrated by the C 1s peak at 284.6 eV arising from adventitious carbon. The Brunauer-Emmett-Teller (BET) surface area and pore size distribution were evaluated by nitrogen sorption at −196 °C using a Quantachrome Autosorb AS-1.

2.3. Catalytic oxidation of phenol solutions

The catalytic oxidation of phenol was employed to probe the efficiency of activation of potassium peroxymonosulfate (Oxone®, $2KHSO_5{\cdot}KHSO_4{\cdot}K_2SO_4$ from Aldrich) and potassium peroxydisulfate ($K_2S_2O_8$ from Sigma-Aldrich). The reactions were carried out in a 500 mL reactor containing 20 ppm of phenol solution. The reactor was attached to a stand and dipped into a water bath with a temperature controller. A catalyst sample at 0.2 g/L was firstly added to the solution and stirred for 10 min. Then PMS or PDS was added to the mixture to start the reaction. The pH of reaction solution was not adjusted, and was about 6.5 at first, then gradually decreased to 2–3 due to the influence from oxidation processes. At each time interval, 1 mL of solution was withdrawn by a syringe and filtered by 0.45 μm Millpore film. The filtered solution was injected into a high performance liquid chromatography (HPLC) vial which was filled with 0.5 mL of methanol as a quenching reagent. Phenol solutions were measured by a HPLC (Varian) with a C-18 column. The adsorption tests were performed without addition of any oxidant.

3. Results and discussion

3.1. Characterization of pristine and N-modified CNTs

Fig. 1(A) shows Raman spectra of pristine and N-CNT-35. For the two samples, D-band at around 1313 cm^{-1} and G-band at around 1579 cm^{-1} were observed. The former band (D-band) originates from the disorder-induced features due to the finite particle size effect, lattice distortion, or amorphous carbon background [27,28]. The G-band arises from the Raman active in-plane atomic displacement E_{2g} mode [29]. The overtone of D band, 2D band, was found at 2633 cm^{-1}. The broad peaks after 2870 cm^{-1} were suggested to be symmetric and asymmetrical C–H stretch vibrations of the CH_3 group and asymmetrical C–H stretch vibrations of the CH_2 group [30]. It was noticed that, after nitrogen modification at temperature of 350 °C, the peak positions were not changed. The ratio (I_D/I_G) of the D-band intensity to the G-band intensity is known to be proportional to the degree of order of carbons [27]. In this study, the I_D/I_G values of pristine CNT and N-CNT-35 were calculated to be 2.06 and 2.01, indicating that nitrogen modification did not significantly change the sp^2 carbon network of the CNT materials. I_D was much higher than I_G, suggesting the faulty long-range ordered crystalline and the existence of disordered carbon structures, as

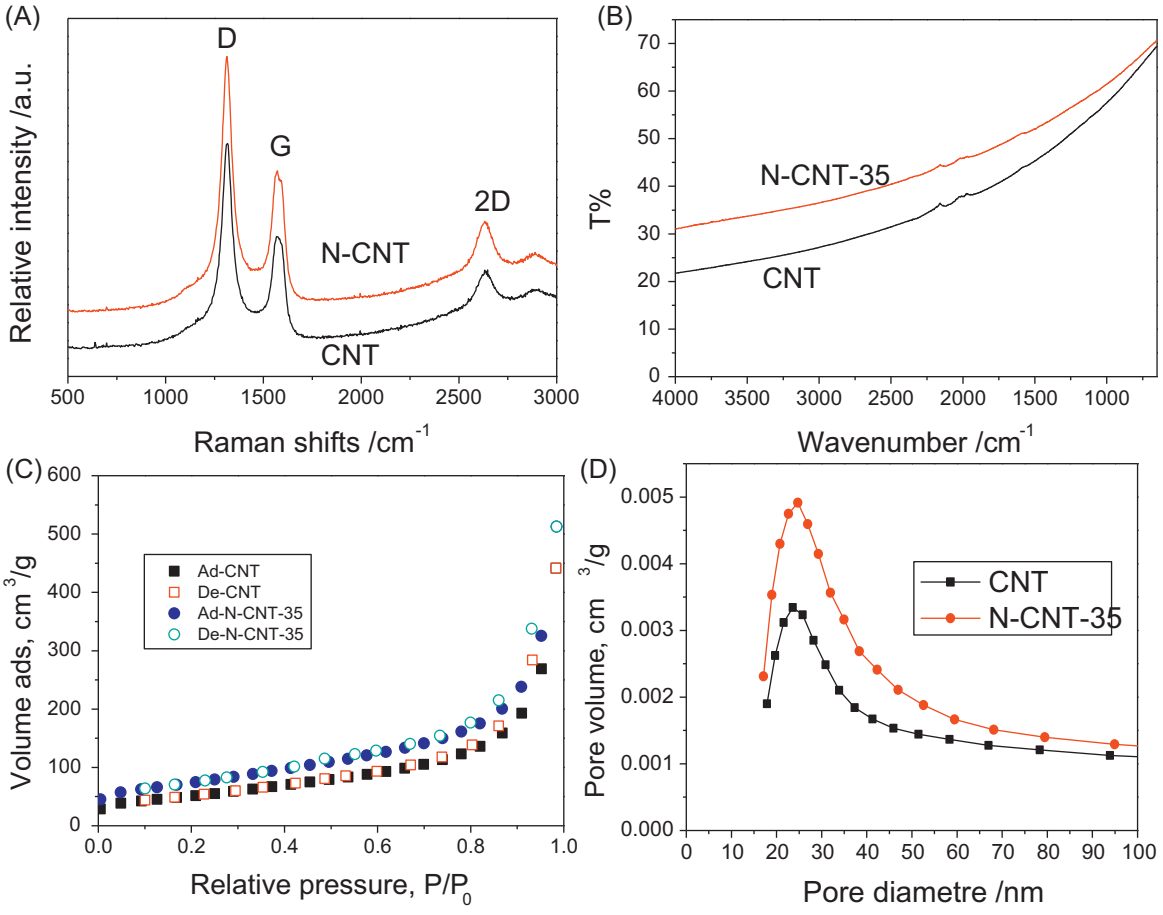

Fig. 1. Raman spectra (A), FTIR spectra (B), N_2 sorption isotherms (C), and pore size distributions (D) of CNT and N-CNT-35.

confirmed by XRD of MWCNT in Fig. S1. Fig. 1(B) presents FTIR spectra of the pristine and N-CNT-35. Neither the N-CNT-35 nor pristine CNT showed strong signals, indicating that no high level of oxygen containing species, such as carboxylic (COOH), carbonyl (C=O) and hydroxyl groups exist [31,32]. This observation will be confirmed by EELS and XPS results shown later. N_2 sorption isotherms and pore size distributions of the pristine and N-CNT-35 are shown in Fig. 1(C) and (D), respectively. The specific surface area (S_{BET}) of unmodified CNT was 187.4 m^2/g, and it was increased to 258.5 m^2/g after nitrogen modification. The gas generation from the decomposition of ammonium nitrate would reduce the aggregation, and then increase the BET of the CNT. A typical type-IV isotherm was observed on the CNTs with a hysteresis loop between $P/P_0 = 0.4–0.9$, indicating the mesoporous structure of the pristine and N-CNT-35 [8,33]. The mesopores centred at around 24 nm were observed on both samples (Fig. 1(D)), suggesting no significant change in porous structure by N-doping.

The morphologies of the CNTs samples are shown in Fig. 2. The pristine sample randomly stacks together, and exhibits significant aggregation. Fig. 2(B) shows SEM image of N-CNT-35. It was found that the tubular structure remained very well after nitrogen modification, due to the low temperature protocol at 350 °C. Fig. S2 shows SEM images of raw CNT, and N-CNT-30, N-CNT-35 and N-CNT-40. The images further confirmed that nitrogen modification did not break the tubular structure of CNT. Fig. 2(C) and (D) show HRTEM images of N-CNT-35, confirmed the nature of multi-walled tube and diameter of 10–20 nm.

FTIR has shown that not many functional groups are present on the pristine and modified CNTs. The chemical compositions of N-CNT-35 were then investigated in-detail. The ratio of carbon, nitrogen and oxygen in the CNTs was estimated from the EEL spectrum taken in an imaging mode [34]. Fig. 3(A) and (B) show the area that the EELS was taken, and the spectrum, respectively. The C:N:O ratio was quantified and the ratios are 90.61 ± 12.2 at% for carbon, 1.52 ± 0.2 at% for nitrogen, and 7.87 ± 1.1 at% for oxygen, respectively. Fig. 3(C) shows XPS survey of the pristine and N-CNT-35. On raw MWCNTs, only carbon and oxygen were detected, and oxygen exists at a very low ratio of 1.54 at%, which was consistent with the FTIR results. After nitrogen modification, the oxygen content increased to 3.30 at%, partially due to the introduction of NO_x species. The nitrogen level was at 0.88 at%, which is not comparable to that of in-situ doping. Chizari et al. [35] reported the synthesis of nitrogen-doped carbon nanotubes using a CVD at temperature ranging from 600 to 850 °C and ethane/ammonia as precursors. The resulting nitrogen doping level was up to 5.5 at%. In another synthesis, when a new precursor of imidazole was used in CVD at 700–950 °C, a high N doping of 12.1–25.7 at% into CNTs was achieved [34]. Sharifi et al. [36] reported that N-CNTs from a CVD using pyridine as the nitrogen precursor had a nitrogen doping level of 9.2 at%. It is known that the nitrogen dopants in nanocarbons can be at different locations, including N atoms doped into a graphene basal plane (quaternary or graphitic N at ca. 401.8 eV), N in a six-membered ring (pyridinic N at ca. 398.3 eV), and a five-membered ring (pyrrolic N at ca. 399.8 eV) [18]. Fig. 3(D) shows XPS N1s spectrum of N-CNT-35. Only pyrrolic and pyridinic N atoms were found, and no graphitic N appeared. This indicated that post-treatment at a low temperature is not able to incorporate nitrogen into the graphitic carbon framework, and the bulk structure of the

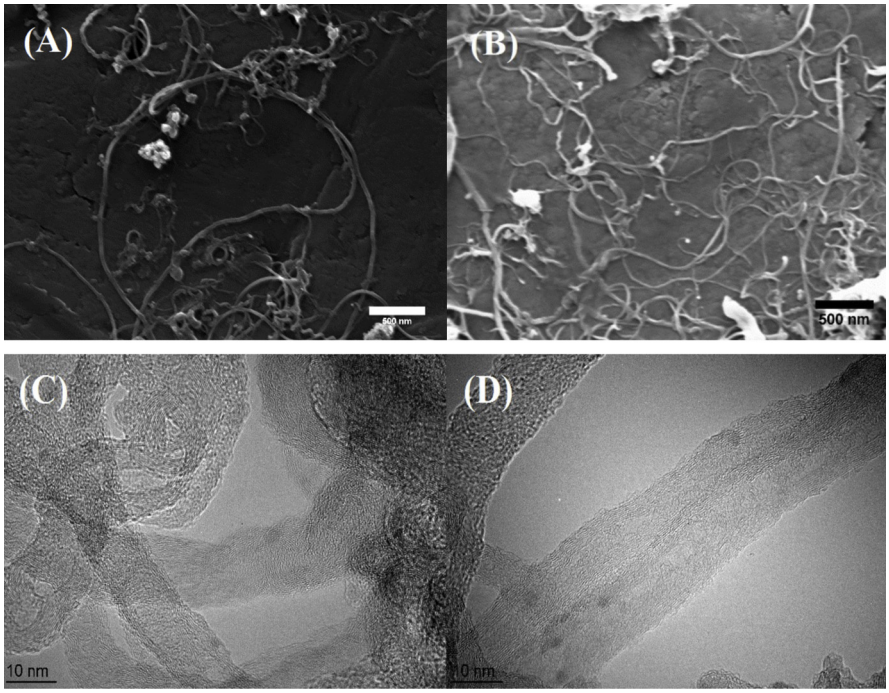

Fig. 2. (A) SEM image of CNT, (B) SEM image of N-CNT, (C) TEM image of N-CNT-35, (D) HRTEM of the tubular structure N-CNT-35.

CNT was not altered [22]. However, the merits of the synthesis in this study are (a) it can employ the commercially available CNTs for a cost-effective synthesis, (b) it is operated at a low temperature for energy-saving preparation, and (c) it offers the opportunity to investigate the effects of surface modification on catalysis without altering the bulk structure. Fig. S3 shows XPS O 1s and C 1s spectra of the N-CNT-35. The low content of oxygen was attributed to the NO_x, hydroxyl (OH) and carbonyl (C=O) groups [37].

3.2. Catalytic oxidation of phenol with PMS on CNTs and N-CNTs

Fig. 4(A) shows the phenol removal at different conditions. The N-CNT-35 was not effective for adsorption of phenol, even though it had larger BET surface area and porosity. That was possibly due to the low concentration of functional groups on the surface. Moreover, without a catalyst, PMS could hardly degrade phenol in solutions. The standard conditions for the catalytic oxidation

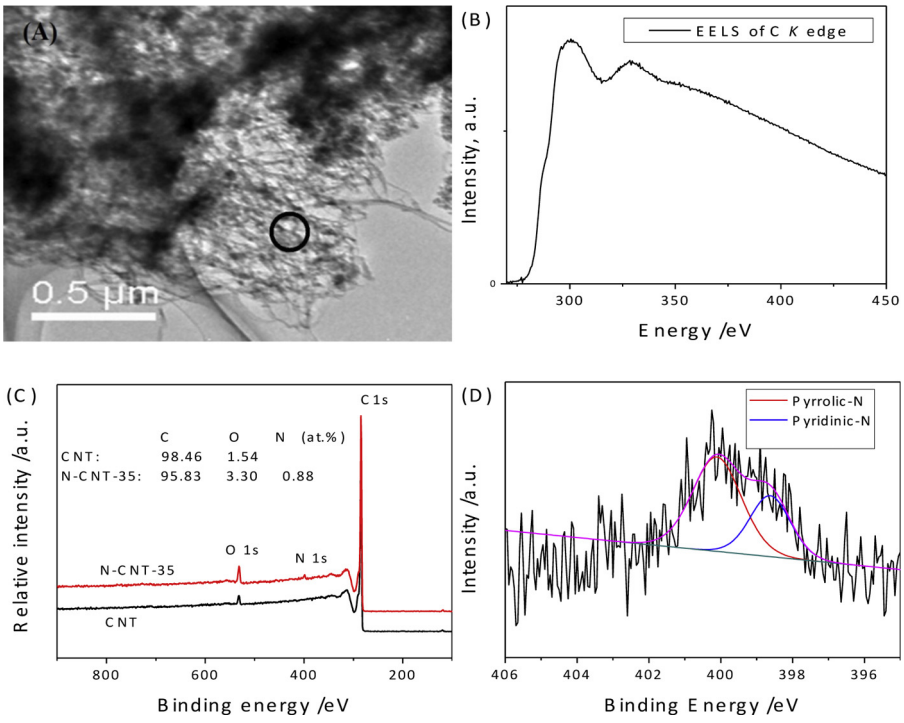

Fig. 3. (A) The area that EELS spectrum taken from, (B) EELS spectrum of N-CNT-35, (C) XPS survey of N-CNT-35, and (D) XPS N1s spectrum of N-CNT-35.

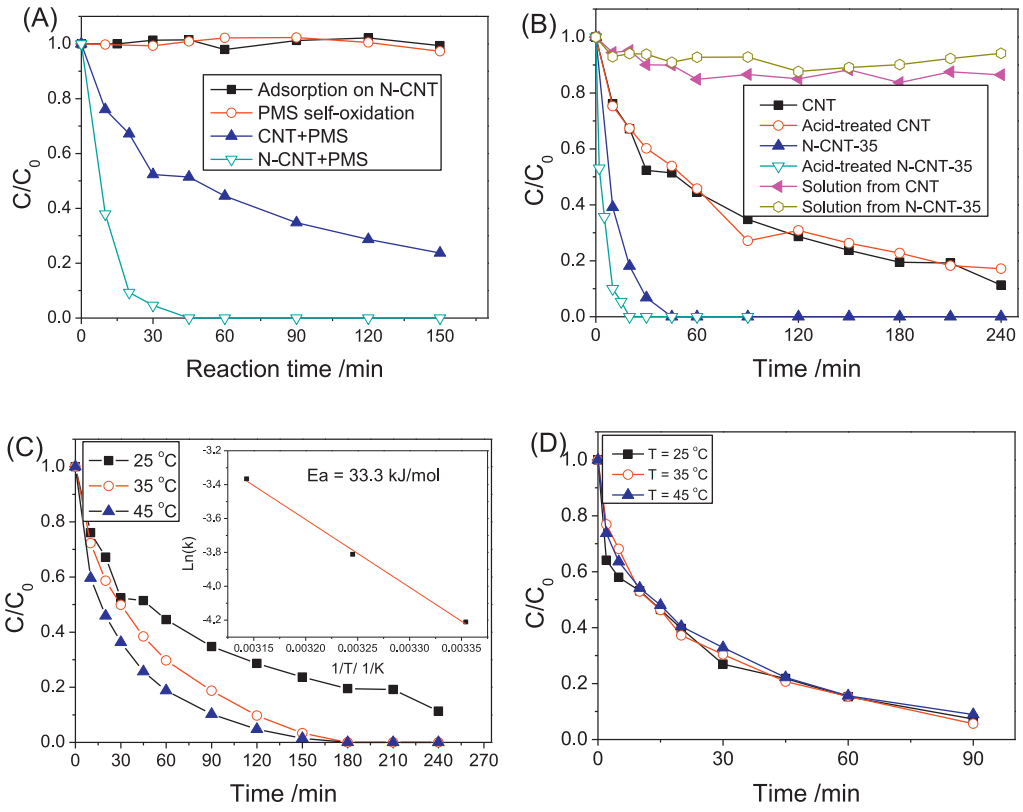

Fig. 4. (A) Phenol removal by different methods, (B) phenol degradation at different conditions, (C) effect of temperature on phenol oxidation on CNT, and (D) effect of temperature on phenol oxidation on N-CNT-35. [Phenol: 20 ppm; Catalyst: 0.2 g/L; Oxone®: 2 g/L; Temperature: 25 °C (standard)].

were: catalyst loading of 0.2 g/L, PMS of 2.0 g/L, phenol solution of 20 ppm, and temperature of 25 °C. It was found that the raw CNTs were able to effectively activate PMS to produce sulfate radicals, then to degrade phenol solutions. In 150 min, about 76% degradation of 20 ppm phenol was achieved. Fig. S4 shows the effects of reaction conditions on the CNTs-catalyzed phenol degradation. As shown in Fig. S4(A), at increased PMS amount, the reaction rate would increase first and then reach the optimal at 2 g/L. Further increasing PMS would not improve the degradation, indicating that a fixed amount of catalyst puts an upper limit on the rate of generation of sulfate radicals [38]. Fig. S4(B) suggests that higher catalyst loading would provide more active sites, and the degradation rate was increased. Fig. S4(C) displays the phenol removals at varying initial concentrations (20, 50 and 100 ppm). Higher initial phenol concentration required a longer time for the same level of phenol removal. In industrial applications, phenol solutions at further higher concentration can be pre-treated by separation for recovery of resources [39].

The nitrogen modification to CNTs can significantly improve the catalytic performance in phenol oxidation. At the same conditions, 100% phenol removal was obtained on N-CNT-35 in 45 min, compared with 76% phenol removal on CNT in 150 min. This degradation efficiency is comparable to that on N-doped rGO [18]. The first-order kinetics was used to describe the reaction, and the rate constants on CNT and N-CNT-35 were estimated to be 0.0136 (R^2 = 0.867) and 0.103 min^{-1} (R^2 = 0.997). The reaction rate of N-CNT-35 was 7.8 times higher than that on CNT. Fig. S5 shows the effect of preparation temperature on the catalytic activity of N-CNTs. It was found that no significant impact occurred at the temperature range, because all these temperatures can induce surface modification, but are not higher enough for the structural change in graphitic N doping.

We further carried out a systematic study to investigate potential effect of metal residue in the commercial CNTs. Fig. 4(B) shows the phenol removal at different conditions. The commercial CNTs and N-CNT-35 were suspended in a 1 M nitric acid solution, stirred overnight, and then washed thoroughly. Due to the low concentration of nitric acid and room temperature treatment, it was unlikely to produce carboxylic groups on the surface of CNTs [40]. As a result, no difference in activity was found on the MWCNT. The acid solutions from the treatment were not effective for activation of PMS, either. Thus, it is indicated that the catalytic activity of pristine CNTs was not attributed to any potential metal residues. It was interesting to find that acid-treatment increased the activity of N-CNT-35, possibly due to the further modification of N-containing dopants and surface charges [41].

The effect of reaction temperature on phenol removal is shown in Fig. 4(C) and (D). On the pristine CNTs, the temperature of reaction solution significantly influenced the degradation rate. Generally, phenol removal would be promoted at the increased reaction temperature. Based on the first-order kinetics, the activation energy of CNT/PMS in the catalytic oxidation of phenol was estimated to be 33.3 kJ/mol using the Arrhenius equation. For a comparison, several activation energies of phenol oxidation on different catalysts were recalled: 59.7 kJ/mol of Co/activated carbon [16], 48.3–62.9 kJ/mol of Co/carbon aerogel [9], 26.5 kJ/mol of Co/reduced graphene oxide [42], 84.9 kJ/mol of reduced graphene oxide [3], 17.6 kJ/mol of activated carbon [43], and 33.3 kJ/mol of CNT (this study). It was shown that CNTs presented a lower activation energy. For the N-CNT-35, it was found that the reaction temperature imposed very slight influence on the degradation. This reaction was not able to be described by the Arrhenius equation. The origin of nitrogen modification to such an effect on N-CNT-35 is still not clear yet.

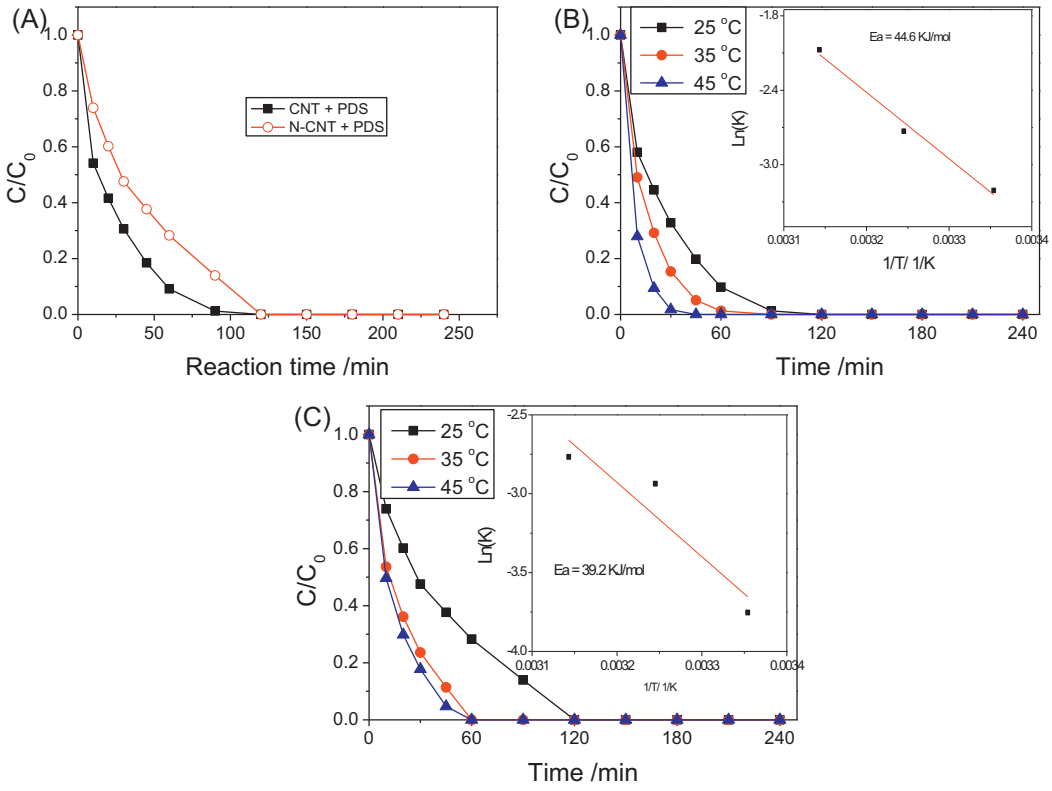

Fig. 5. (A) Phenol degradation on CNT and N-CNT-35 with PDS, (B) effect of temperature on phenol oxidation on CNT, and (C) effect of temperature on phenol oxidation on N-CNT-35. [Phenol: 20 ppm; Catalyst: 0.2 g/L; PDS: 1.48 g/L; Temperature: 25 °C (standard)].

3.3. Catalytic oxidation of phenol with PDS on CNTs and N-CNTs

Fig. 5(A) shows the catalytic oxidation of phenol on CNT and N-CNT-35 with PDS. The standard conditions for the catalytic oxidation were: catalyst loading of 0.2 g/L, PDS of 1.48 g/L (maintaining the same mole of sulfate radicals with 2 g/L of PMS), phenol solution of 20 ppm, and temperature of 25 °C. In 90 min reaction, the pristine CNT almost removed 100% phenol. Meanwhile, the nitrogen modified CNT needed 120 min to achieve 100% phenol degradation with PDS. When fitted by the first-order kinetics, the reaction rate constants of CNT and N-CNT-35 were estimated to be 0.0439 (R^2 = 0.972) and 0.0234 min^{-1} (R^2 = 0.983). The pristine CNT showed 1.88 times higher activity than N-CNT-35 in the activation of PDS for phenol oxidation. Fig. S6 shows the kinetic studies of phenol oxidation on CNT with PDS at varying CNT, PDS and phenol concentrations, and the results were similar to those with PMS.

Fig. 5(B) and (C) show the effect of reaction temperature on the phenol catalytic oxidation. On pristine CNT, 100% phenol removal required 90 min at 25 °C, and the time was reduced to 45 min when the temperature was increased to 45 °C. The activation energy of CNT in the activation of PDS for phenol degradation was calculated to be 44.6 kJ/mol. On the N-CNT-35, 100% phenol removal at 25 °C needed 120 min. When the reaction temperature was increased to 45 °C, the complete phenol removal reached at 60 min. The activation energy of N-CNT-35 in phenol degradation by activation of PDS was 39.2 kJ/mol.

3.4. Mechanism of nitrogen modification of CNTs on the activation of PMS and PDS

Analysis of the chemical compositions of CNT and N-CNT-35 by XPS, EELS and FTIR indicated that the pristine CNT had a very low level of oxygen, mainly as hydroxyl and carbonyl groups, at the ends of the tubes. Carbon in rolled graphene sheets is very stable [44]. When annealed with ammonium nitrate at low temperatures, the produced ammonia would react with the defects at the ends of the tubes, other than the rolled graphene sheets. As shown in XPS, pyridinic and pyrrolic N would be produced. Scheme 1 shows the structure of CNT with carbonyl and hydroxyl groups and the modification by pyridinic and pyrrolic N. This is different from our recent study, in which graphitic N was formed in rGO by the similar protocol [18]. However, the nanocarbon precursor of rGO was GO, which is not stable and would undergo a process to rebuild its graphene sheets. In doping process, N was able to be doped into graphene sheets. However, Raman, SEM and XPS results in this study show that the bulk properties of CNT were not changed before and after nitrogen modification, suggesting that the nitrogen atoms were only located at the defective sites of the carbon nanotubes.

Since the discovery of the catalytic activity of nanocarbons in activation of PMS [3], systematic studies have been conducted to illustrate the catalytically active sites. The comparison of GO and rGO indicated that sp^2 carbon and oxygen-containing groups mainly contribute to the catalytic activity [3]. In the subsequent study of structural modification of rGO, we proved that the catalytic activity was not related to the specific surface area, but to the concentration of oxygen-containing groups [17]. In a recent study, nitrogen doped rGO was demonstrated to be more active, and almost 30 times higher activity was achieved than rGO via the same preparation [18]. The modification of sp^2 carbon by graphitic N doping and N atoms at defective sites were attributed to the greatly improved activity.

In this study, the activity of pristine CNT was mainly attributed to sp^2 carbon and functional groups. On N-CNT, sp^2 carbon and functional groups still worked as active sites. From XPS, no graphitic N was produced, and the influence of activated π electrons by N doping to sp^2 carbon was eliminated. The significant improvement

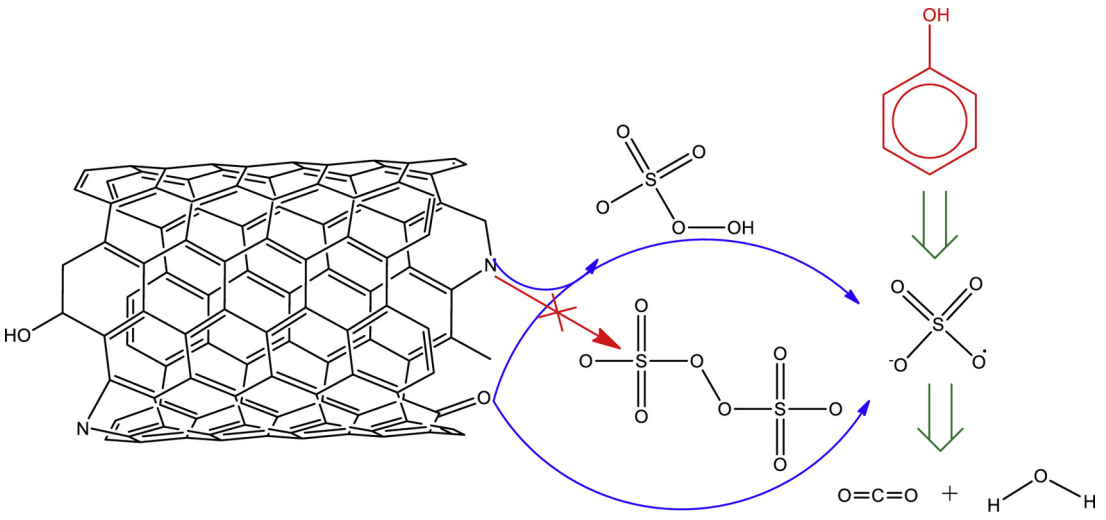

Scheme 1. Nitrogen modified CNTs in activation of PMS and PDS for phenol oxidation.

of the catalytic activity of N-CNT in PMS activation was then attributed to the introduced pyridinic and pyrrolic N atoms. It is noteworthy that the N doping level was very low (0.88 at%), then the 7.8 times of activity improvement strongly suggested that pyridinic and pyrrolic N dopants are much more active than oxygen-containing functional groups. Scheme 1 schematically shows the activation processes of PMS and the followed oxidation of phenol into water and carbon dioxide. Fig. 4(B) shows that acid-treatment of N-CNT-35 would increase the catalytic activity. The reason might be that nitrogen modification changed the surface charges of the CNT by forming NO_x groups from ammonium nitrate decomposition, and the further acid-treatment would clean up the active sites covered by those groups. Similar improvement by acid washing was found on NO_x modified titanium dioxide in photocatalysis [41].

PDS activation seems to be different from PMS. As shown in Scheme 1, nitrogen dopants were not effective for PDS activation, which can only be induced by sp^2 carbon and functional oxygen groups. Upon nitrogen modification, the effective groups, such as C=O were partially replaced by non-effective NO_x groups, or pyridinic and pyrrolic N. Therefore, the activity of N-CNT in activation of PDS was decreased and became lower than the pristine CNT.

Table 1 lists the different methods for activation of PMS and PDS. In general, PDS and PMS can be activated by the same methods, such as heat, UV, electron and metal ions, yet the effectiveness varies on different compounds/methods. For example, Ag^+ is very effective for PDS activation, while Co^{2+} is effective for PMS activation. Organic compounds were found to be effective for PDS, and on the other hand, anions were effective for PMS. The nature of PDS and PMS activation lies in the processes of breaking SO–OS of PDS and O–OH of PMS, controlled by both the binding energy of the bonds and the ability of catalyst in transferring electrons to the bonds in PDS and PMS. Therefore, in this study it is showed both CNT-C=O and CNT-C=N can transfer electron to PMS for producing sulfate radicals, while only CNT-C=O is effective for PDS activation. It is noteworthy that the stability of the active sites of nanocarbons is not as high as a metal-based catalyst, so the reusability of N-CNT catalysts was still low and further research is being carried out (SI, Fig. S7).

Table 1
Activation of PMS and PDS by different methods.

Activation	PDS	PMS	References
Heat	$S_2O_8^{2-} + heat \rightarrow 2SO_4^{-\bullet}$	$HSO_5^- + heat \rightarrow SO_4^{-\bullet} + OH^-$	[45,46]
UV ($h\nu$)	$S_2O_8^{2-} + h\nu \rightarrow 2SO_4^{-\bullet}$	$HSO_5^- + h\nu \rightarrow SO_4^{-\bullet} + OH^-$	[45,46]
Electron	$S_2O_8^{2-} + e^- \rightarrow SO_4^{-\bullet} + SO_4^{2-}$	$HSO_5^- + e^- \rightarrow SO_4^{-\bullet} + OH^-$	[46,47]
Metal ions	$S_2O_8^{2-} + M^{n+}$ (Ag^+, Fe^{2+}, Cu^+) $\rightarrow M^{(n+1)+} + SO_4^{-\bullet} + SO_4^{2-}$	$HSO_5^- + M^{n+}$ (Co^{2+}, Ru^{3+}, Fe^{2+}, Mn^{2+}) $\rightarrow M^{(n+1)+} + SO_4^{-\bullet} + OH^-$	[4,11,45,46,48,49]
Base	$2S_2O_8^{2-} + 2H_2O \rightarrow 3SO_4^{2-} + SO_4^{-\bullet} + 4H^+ + O_2^{-\bullet}$	N/A	[50]
Activated carbon (AC)	AC surface-OOH + $S_2O_8^{2-} \rightarrow SO_4^{-\bullet}$ + AC surface-OO• + HSO_4^-; AC surface-OOH + $S_2O_8^{2-} \rightarrow SO_4^{-\bullet}$ + AC surface-O• + HSO_4^-	$AC + HSO_5^- \rightarrow AC^+ + SO_4^{-\bullet} + OH^-$	[43,51]
Phenols	$PhO^- + S_2O_8^{2-} \rightarrow SO_4^{-\bullet} + SO_4^{2-} + PhO_{ox}$	N/A	[52]
Quinone (Q) and hydroquinone (H_2Q)	$Q + H_2Q \rightarrow 2SQ^{-\bullet} + 2H^+$; $SQ^{-\bullet} + S_2O_8^{2-} \rightarrow SO_4^{-\bullet} + Q + SO_4^{2-}$	N/A	[53]
Anions	N/A	HSO_3^- (or CO_3^{2-}, HCO_3^-, HPO_4^{2-}, Cl^-) + $HSO_5^- \rightarrow SO_4^{-\bullet} + SO_3^{-\bullet} + H_2O$	[54]
rGO	N/A	rGO-C=O + $HSO_5^- \rightarrow$ rGO-C-O* + $SO_4^{-\bullet} + OH^-$	[3]
N-rGO	N/A	rGO-C=N + $HSO_5^- \rightarrow$ rGO-C–N* + $SO_4^{-\bullet} + OH^-$	[18]
CNT and N-CNT	CNT-C=O + $S_2O_8^{2-} \rightarrow$ CNT-C-O* + $SO_4^{-\bullet} + SO_4^{2-}$	CNT-C=O + $HSO_5^- \rightarrow$ CNT-C–O* + $SO_4^{-\bullet} + OH^-$; CNT-C=N + $HSO_5^- \rightarrow$ CNT-C–N* + $SO_4^{-\bullet} + OH^-$	This study

4. Conclusions

Commercial MWCNTs are able to effectively activate PMS and PDS to produce sulfate radicals for catalytic oxidation of phenol solutions. A facile post-treatment of raw CNTs by nitrogen modification were able to significantly increase the catalytic activity in phenol oxidation with PMS by a 7.8-fold enhancement. However, nitrogen modification posed a negative effect on PDS activation. The mechanistic study facilitated by the advanced characterizations and the catalytic reactions suggested that both sp^2 carbon and oxygen-containing groups would contribute to the activity in PMS and PDS activation on the pristine CNTs. Nitrogen dopants are much more active than the oxygen-containing groups for PMS activation, however, they are not effective for PDS activation. This study demonstrates a metal-free material for wastewater treatment by means of sustainable remediation, and also suggests a facile approach to significantly improve the catalytic activity of carbon materials.

Acknowledgments

This work was financially supported by Australian Research Council (DP130101319). The authors acknowledge the use of equipment, scientific and technical assistance of the Curtin University Electron Microscope Facility and Centre for Microscopy Characterization and Analysis at The University of Western Australia, which have been partially funded by the University, State and Commonwealth Governments.

Appendix A. Supplementary data

Supplementary data associated with this article can be found, in the online version, at http://dx.doi.org/10.1016/j.apcatb.2014.02.012.

References

[1] G.P. Anipsitakis, D.D. Dionysiou, Environ. Sci. Technol. 37 (2003) 4790–4797.
[2] P. Shukla, H.Q. Sun, S.B. Wang, H.M. Ang, M.O. Tade, Catal. Today 175 (2011) 380–385.
[3] H.Q. Sun, S.Z. Liu, G.L. Zhou, H.M. Ang, M.O. Tade, S.B. Wang, ACS Appl. Mater. Interfaces 4 (2012) 5466–5471.
[4] G.P. Anipsitakis, D.D. Dionysiou, Environ. Sci. Technol. 38 (2004) 3705–3712.
[5] G.P. Anipsitakis, D.D. Dionysiou, M.A. Gonzalez, Environ. Sci. Technol. 40 (2006) 1000–1007.
[6] E. Saputra, S. Muhammad, H.Q. Sun, H.M. Ang, M.O. Tade, S.B. Wang, Environ. Sci. Technol. 47 (2013) 5882–5887.
[7] E. Saputra, S. Muhammad, H.Q. Sun, H.M. Ang, M.O. Tade, S.B. Wang, Appl. Catal., B 142 (2013) 729–735.
[8] H.Q. Sun, G.L. Zhou, S.Z. Liu, H.M. Ang, M.O. Tade, S.B. Wang, ACS Appl. Mater. Interfaces 4 (2012) 6235–6241.
[9] H.Q. Sun, H.Y. Tian, Y. Hardjono, C.E. Buckley, S.B. Wang, Catal. Today 186 (2012) 63–68.
[10] W. Zhang, H.L. Tay, S.S. Lim, Y.S. Wang, Z.Y. Zhong, R. Xu, Appl. Catal., B 95 (2010) 93–99.
[11] C.J. Liang, Y.Y. Guo, Environ. Sci. Technol. 44 (2010) 8203–8208.
[12] H.Q. Sun, H.W. Liang, G.L. Zhou, S.B. Wang, J. Colloid Interface Sci. 394 (2013) 394–400.
[13] J. Luo, F. Peng, H. Yu, H.J. Wang, W.X. Zheng, ChemCatChem 5 (2013) 1578–1586.
[14] J. Zhang, D.S. Su, A.H. Zhang, D. Wang, R. Schlogl, C. Hebert, Angew. Chem. Int. Ed. 46 (2007) 7319–7323.
[15] J. Pyun, Angew. Chem. Int. Ed. 50 (2011) 46–48.
[16] P.R. Shukla, S.B. Wang, H.Q. Sun, H.M. Ang, M. Tade, Appl. Catal., B 100 (2010) 529–534.
[17] W.C. Peng, S.Z. Liu, H.Q. Sun, Y.J. Yao, L.J. Zhi, S.B. Wang, J. Mater. Chem. A 1 (2013) 5854–5859.
[18] H. Sun, Y. Wang, S. Liu, L. Ge, L. Wang, Z. Zhu, S. Wang, Chem. Commun. 49 (2013) 9914–9916.
[19] X.M. Ren, C.L. Chen, M. Nagatsu, X.K. Wang, Chem. Eng. J. 170 (2011) 395–410.
[20] J. Zhang, X. Liu, R. Blume, A.H. Zhang, R. Schlogl, D.S. Su, Science 322 (2008) 73–77.
[21] H. Yu, F. Peng, J. Tan, X.W. Hu, H.J. Wang, J.A. Yang, W.X. Zheng, Angew. Chem. Int. Ed. 50 (2011) 3978–3982.
[22] D.S. Yu, E. Nagelli, F. Du, L.M. Dai, J. Phys. Chem. Lett. 1 (2010) 2165–2173.
[23] K. Chizari, A. Deneuve, O. Ersen, I. Florea, Y. Liu, D. Edouard, I. Janowska, D. Begin, P.H. Cuong, ChemSusChem 5 (2012) 102–108.
[24] J. Luo, F. Peng, H.J. Wang, H. Yu, Catal. Commun. 39 (2013) 44–49.
[25] L.Y. Feng, Y.Y. Yan, Y.G. Chen, L.J. Wang, Energy Environ. Sci. 4 (2011) 1892–1899.
[26] T. Thurakitseree, C. Kramberger, A. Kumamoto, S. Chiashi, E. Einarsson, S. Maruyama, ACS Nano 7 (2013) 2205–2211.
[27] Y. Lu, Z.P. Zhu, Z.Y. Liu, Carbon 42 (2004) 361–370.
[28] G.M. Neelgund, A. Oki, Appl. Catal., B 110 (2011) 99–107.
[29] X.F. Xie, L. Gao, Carbon 45 (2007) 2365–2373.
[30] Y.L. Liu, C.X. Pan, J.B. Wang, J. Mater. Sci. 39 (2004) 1091–1094.
[31] G.D. Vukovic, A.D. Marinkovic, M. Colic, M.D. Ristic, R. Aleksic, A.A. Peric-Grujic, P.S. Uskokovic, Chem. Eng. J. 157 (2010) 238–248.
[32] T.A. Saleh, S. Agarwal, V.K. Gupta, Appl. Catal., B 106 (2011) 46–53.
[33] D.G. Tong, W. Chu, P. Wu, G.F. Gu, L. Zhang, J. Mater. Chem. A 1 (2013) 358–366.
[34] K. Ghosh, M. Kumar, T. Maruyama, Y. Ando, J. Mater. Chem. 20 (2010) 4128–4134.
[35] K. Chizari, I. Janowska, M. Houlle, I. Florea, O. Ersen, T. Romero, P. Bernhardt, M.J. Ledoux, C. Pham-Huu, Appl. Catal., A 380 (2010) 72–80.
[36] T. Sharifi, F. Nitze, H.R. Barzegar, C.W. Tai, M. Mazurkiewicz, A. Malolepszy, L. Stobinski, T. Wagberg, Carbon 50 (2012) 3535–3541.
[37] R.H. Bradley, K. Cassity, R. Andrews, M. Meier, S. Osbeck, A. Andreu, C. Johnston, A. Crossley, Appl. Surf. Sci. 258 (2012) 4835–4843.
[38] P. Shukla, S.B. Wang, K. Singh, H.M. Ang, M.O. Tade, Appl. Catal., B 99 (2010) 163–169.
[39] G. Busca, S. Berardinelli, C. Resini, L. Arrighi, J. Hazard. Mater. 160 (2008) 265–288.
[40] V. Datsyuk, M. Kalyva, K. Papagelis, J. Parthenios, D. Tasis, A. Siokou, I. Kallitsis, C. Galiotis, Carbon 46 (2008) 833–840.
[41] H.Q. Sun, Y. Bai, H.J. Liu, W.Q. Jin, N.P. Xu, G.J. Chen, B.Q. Xu, J. Phys. Chem. C 112 (2008) 13304–13309.
[42] Y.J. Yao, Z.H. Yang, H.Q. Sun, S.B. Wang, Ind. Eng. Chem. Res. 51 (2012) 14958–14965.
[43] E. Saputra, S. Muhammad, H. Sun, S. Wang, RSC Adv. 3 (2013) 21905–21910.
[44] D.P. He, Y.L. Jiang, H.F. Lv, M. Pan, S.C. Mu, Appl. Catal., B 132 (2013) 379–388.
[45] R.H. Waldemer, P.G. Tratnyek, R.L. Johnson, J.T. Nurmi, Environ. Sci. Technol. 41 (2007) 1010–1015.
[46] G.L. Zhou, H.Q. Sun, S.B. Wang, H.M. Ang, M.O. Tade, Sep. Purif. Technol. 80 (2011) 626–634.
[47] C.J. Liang, C.F. Huang, Y.J. Chen, Water Res. 42 (2008) 4091–4100.
[48] H.Y. Liang, Y.Q. Zhang, S.B. Huang, I. Hussain, Chem. Eng. J. 218 (2013) 384–391.
[49] M. Sundar, D. Easwaramoorthy, S.K. Rani, I.M. Bilal, Catal. Commun. 9 (2008) 2340–2344.
[50] O.S. Furman, A.L. Teel, R.J. Watts, Environ. Sci. Technol. 44 (2010) 6423–6428.
[51] S.Y. Yang, X. Yang, X.T. Shao, R. Niu, L.L. Wang, J. Hazard. Mater. 186 (2011) 659–666.
[52] M. Ahmad, A.L. Teel, R.J. Watts, Environ. Sci. Technol. 47 (2013) 5864–5871.
[53] G.D. Fang, J. Gao, D.D. Dionysiou, C. Liu, D.M. Zhou, Environ. Sci. Technol. 47 (2013) 4605–4611.
[54] S.Y. Yang, P. Wang, X. Yang, L. Shan, W.Y. Zhang, X.T. Shao, R. Niu, J. Hazard. Mater. 179 (2010) 552–558.